Ceramics International **22** (1996) 359–364

0272-8842(95)00085-2
0272-8842/96/$15.00

Superconducting High-T_c Electronic Devices

A. Barone,[a] S. Barbanera,[b] V. Boffa,[c] G. Filatrella,[d] U. Gambardella,[ce] S. Matarazzo[d] & S. Pagano[d]

[a]INFM-Dipartimento di Scienze Fisiche, Università di Napoli "Federico II", P. Tecchio, 80, 80125, Napoli, Italy

[b]Istituto di Elettronica dello Stato Solido, CNR, Via Cineto Romano 42, 00156, Roma, Italy

[c]ENEA CRE Frascati, Via E. Fermi 27, 00044, Frascati, Italy

[d]Istituto di Cibernetica, CNR, Via Toiano 6, 80072, Arco Felice, Italy

[e]Permanent address: INFN-LNF, P.O. Box 13, 00044RM, Frascati, Italy

(Received 7 July 1995; accepted 1 August 1995)

Abstract: The potential applications of high-T_c ceramic superconducting materials is a subject of intensive investigation in many laboratories worldwide. In this paper, results concerning devices based on Josephson junctions, SQUIDs and arrays are presented. © 1996 Elsevier Science Limited and Techna S.r.l.

1 INTRODUCTION

The relatively high critical temperature which characterizes ceramic superconductors offers a chance in the context of both small (electronics) and large (electrotechnical) applications. We shall confine ourselves to the former category, namely superconductive electronics and, more specifically, to active devices.

Although the prospect of less restrictive requirements of the cryogenic enviroment is quite attractive, the difficulty of realizing reliable devices, as well as the severe prescriptions posed by a variety of applications with respect to the thermal noise level, remain challenging iusses in the research in high-T_c components.

Anyway, competitiveness of the high-T_c superconductors widely justifies the efforts toward both basic and applied research in the field.

In this paper we shall outline the main ideas concerning two aspects of research activity carried out in cooperation by our laboratories. Far from the being exhaustive, the discussion will be devoted to two issues of great interest for high-T_c devices, namely SQUIDs and microwave generators.

Section 2 deals with the realization of SQUIDs using YBCO junctions of step-edge type, while Section 3 describes research activity developed in connection with the dynamics of fluxons in high-T_c junctions arrays. Conclusions and perspectives are summarized in Section 4.

2 DC SQUIDS BASED ON YBCO STEP-EDGE JUNCTIONS

The realization of Josephson junctions in the sandwich film configuration, such as those made by low-T_c superconductors is a very hard task. Indeed, the quality of the barrier interfaces in a high-T_c structure is set by the extremely short coherence length of these materials. Therefore, in view of actual active devices, a variety of weakly coupled superconducting structures have been investigated.[1] Among the various configurations, the step-edge junction seems to be very promising.[2]

2.1 SQUID fabrication

To realize sharp steps a 500 nm thick Nb film is first deposited on the substrates ($SrTiO_3$, $LaAlO_3$

and MgO, [100] orientation, 7.5 x 7.5 mm^2) by means of dc magnetron sputtering. The Nb mask is subsequently defined by photolithography and reactive ion etching (RIE) in CF_4. Substrates are then placed on a water-cooled substrate holder at a distance of 10 cm from a 2.54 cm Kaufman type ion source. An Ar^+ beam (400 eV and 10^{-3} A/cm^2) impinging on the substrate at an angle of 30° at a pressure of 0.112 Pa makes a 200 nm deep step in 10 min. The Nb mask is subsequently removed by RIE. Typical step angles are between 60° and 70°. Then substrates are annealed at 1100°C for 4 h in flowing oxygen in order to recover from possible surface damage due to ion bombardment.

The YBCO superconducting film is grown *in situ* by laser ablation.[3] A 308 nm pulsed XeCl excimer laser, having an energy density of 2 J/cm^2, is used with a repetition rate of 10 Hz. The substrate temperature and oxygen pressure during deposition are 760°C and 225 mTorr, respectively. Films have been grown to a thickness roughly equal to the step depth. Soon after deposition the chamber is filled with oxygen up to a pressure of 400 Torr and the sample is cooled at a rate of 10°C/min. In this way epitaxial *c*-axis oriented films with T_c in the range of 88–90 K, and critical current densities at 77 K of 6×10^5 A/cm^2 are obtained.

The pattern on the YBCO film is realized by standard photolithographic techniques. To get the final pattern the ion etching process has been used, as chemical wet etching is less suitable for precise pattern definition, due to unavoidable under-etching. The ion beam parameters are the same as for the step fabrication, but the incidence angle is 0° to minimize shadow effects, which occur when structure sizes are comparable to the resist mask thickness. Furthermore, the sample is glued by means of silver paint on to the water-cooled sample holder to prevent the resist from being overbaked by the energetic Ar ions.

In Fig. 1 the picture of typical SQUID geometry is shown after completion of the patterning process; the two constrictions, 1.8 μm wide and 8 μm long, are aligned perpendicular to the step in the substrate. The substrate step can be easily seen running across the SQUID loop and the two YBCO narrow bridges.

2.2 Measurements

The devices are tested using a liquid helium cryogenic system capable of keeping the sample temperature stable within 0.01 K in the temperature interval (4.2–300) K. The cryogenic insert, which also includes the front-end electronics, allows testing of several devices without cycling to room temperature. The liquid helium dewar is magnetically shielded by a specially designed container made of three layers of μ-metal and a 1 cm thick Al layer to achieve effective screening against the Earth's magnetic field and rf interference. Current–voltage (I–V) characteristics of the devices, as well as their magnetic field behaviour, are recorded using computer controlled equipment.

Fig. 1. Typical dc SQUID optical microscope image. The step is across the constrictions.

Experimental data concerning two different devices realized on $SrTiO_3$ and MgO substrates, respectively, both with orientation [100], are shown. The steps are 150 nm deep with a slope of 70° and 260 nm with a slope of 60° for the $SrTiO_3$ and MgO substrates, respectively. The YBCO film thickness is 250 nm in the former case and 450 nm in the latter case. The critical current density in the weak links is in the range 10^3 A/cm^2 at 77 K in both cases. Figure 2 shows the I–V characteristics for the SQUID realized on MgO substrate recorded at different temperatures. The critical currents of the parallel junctions range from 2.5 mA at 4.2 K to 10 μA at 79 K. As can be seen, in some cases the curves show asymmetries, hystereses and instabilities strongly affected by either external magnetic field or temperature variation. However, since this hysteretic behaviour is non-symmetrical in the positive and negative branches and dependent on the value of the external magnetic field, it is difficult to ascribe it to self-heating phenomena.

This behaviour ceases at $T \approx 79$ K when thermal noise totally conceals these structures. When the SQUID is current-biased in the temperature range $T \approx 60$ K the I–V curve is similar to the one generated by a Resistively Shunted Junction (RSJ) model.[4] In this case the voltage shows regular and reproducible modulations with magnetic field. Figure 3 shows the SQUID voltage as a function

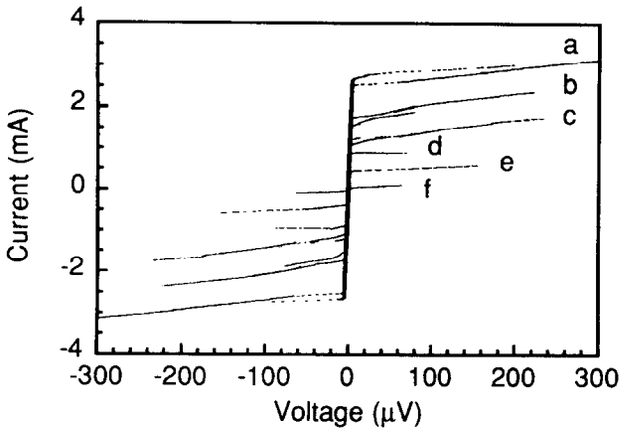

Fig. 2. I–V characteristics of a SQUID device realized on MgO at different temperatures: (a) T = 4.2 K; (b) T = 35 K; (c) T = 50 K; (d) T = 59 K; (e) T = 70 K; (f) T = 79 K.

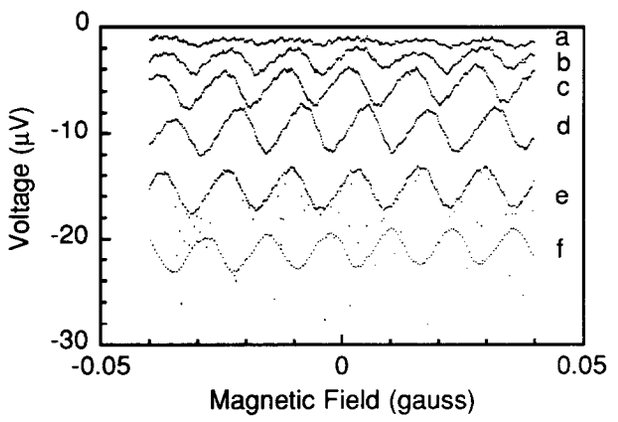

Fig. 3. Voltage modulation of the YBCO dc SQUID in an applied magnetic field at $T \approx 60$ K. The curves correspond to different bias currents: (a) $I = -850$ μA; (b) $I = -870$ μA; (c) $I = -880$ μA; (d) $I = -890$ μA; (e) $I = -900$ μA; (f) $I = -930$ μA.

of the applied magnetic field for different bias currents at 60 K. The magnetic field periodicity is 14 mG, which is consistent with the SQUID geometry (loop area = 16 × 16 μm^2) and a flux focusing factor of ≈ 6. Similar results are obtained for the SQUID made on $SrTiO_3$ with a loop area of 8 × 8 μm^2; the periodicity in this case is 57 mG and the flux focusing factor is again 6.

The presence of structures and branches on the I–V characteristics in certain voltage regions could be due to the presence of multiple junctions in the step region. The distributed properties of the junctions, such as critical current and normal resistance, generate metastable states corresponding to different trapped magnetic field and flowing current configurations. In addition, fluctuations due to external noise and bath temperature can randomly induce jumps between different states resulting in the noisy branches often observed in the I–V curves of the samples. The statistical nature of the junction clusters allows that, for some temperature, magnetic field, and bias current ranges, the whole junction cluster behaves like a single junction and the typical SQUID periodic response is observed. This hypothesis is supported by the presence of structures only in the samples on MgO substrates, where the YBCO film tends to form grain boundaries along the step.

3 FLUXON DYNAMICS IN HIGH-T_C JOSEPHSON JUNCTIONS ARRAY

Fluxon propagation in long Josephson junction has been widely investigated over the years, both as a model system for soliton dynamics[5] and in sight of possible practical applications,[6] such as local oscillator for SIS mixers and flux-flow amplifiers.[7]

A one-dimensional fluxon oscillator is based on a Josephson junction which is much longer than the Josephson penetration depth, λ_j, in one direction and comparable to or less than λ_j in the other one. In this case, if the junction is properly dc-biased, a soliton (which is basically a fluxon) can oscillate back and forth in the junction, and when it impinges on the free end of the junction causes the emission of a pulse of electromagnetic energy. If the arrival of the soliton at the end of the junction is time-periodic, so is the radiation emitted. For typical experimental junctions made with currently available fabrication technologies (based on low critical temperature materials) this frequency of radiation lies within the microwave to millimetre-wave region of the electromagnetic spectrum, with a power in the low nW range. This power, however, is too low for most applications.

It is possible to raise the power of the oscillator by using one- or two-dimensional arrays of resonant propagation oscillators.[8–10]

In this section we focus our attention on a system consisting of a one-dimensional array of high-T_c coupled Josephson junctions, designed to generate microwave radiation through controlled fluxon dynamics.

In Fig. 4(a) is shown a microphotograph of a preliminary YBCO device. It consists of three basic elements: (1) an array of coupled Josephson junctions, each appearing as a small microbridge (2μm size) defined on polycrystalline YBCO film; (2) a control line (on the left of the device) generating a local magnetic field when a current I_L is passing through it; (3) a detector junction (on the right of the device) which is coupled to the array through an Au resistor R_s.

The electrical model of the device is shown in Fig. 4(b), where additional current control inputs

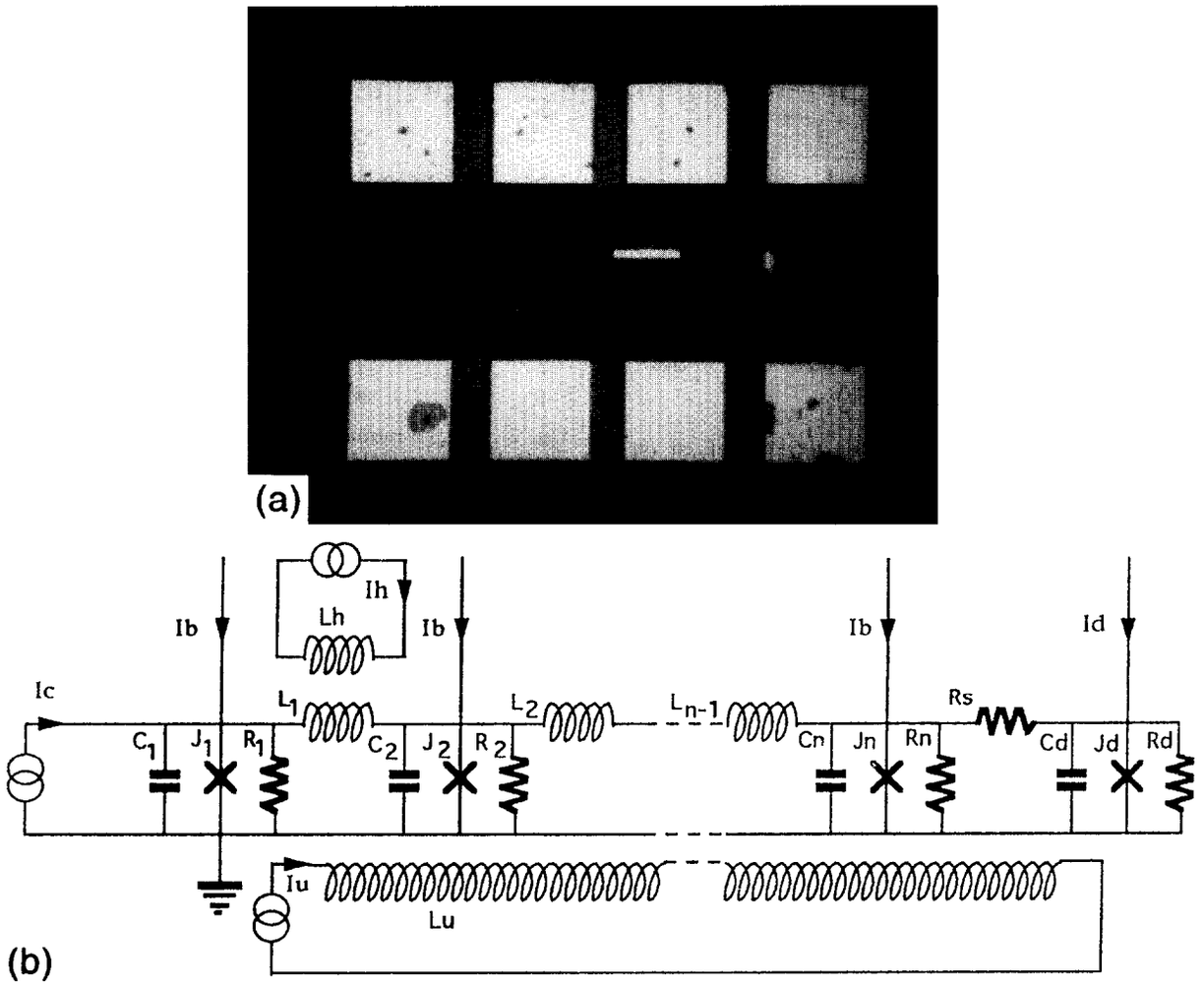

Fig. 4. (a) Microphotograph of the proposed device. (b) Its electrical model.

have been considered: I_c as an additional current bias for the first junction of the array, and I_u which generates a magnetic field uniformly coupled to the array. Junctions are modelled by the usual RSJ model, which well describes both SIS and SNS type junctions. The bias current I_b is supposed to be spatially uniform. For the sake of simplicity we will assume that all the junctions are equal, as well as all the loop inductances.

By writing the equation for the current in each junction, taking into account the flux quantization[4] in the superconducting loop, and applying the usual normalization, a set of coupled ordinary differential equations[11] describing the time evolution of the phase Φ in the N junctions in the array and of the detector are obtained.

These equations are numerically integrated using parameters close to the experimentally reasonable values. In particular, high damping configurations ($a = 1/RC\omega_p = 1$, where ω_p is the plasma frequency) typical of high-T_c superconductors devices have been investigated.

3.1 Numerical results

Figure 5 shows a typical result of an array simulation. The figure shows a 3-D plot of the voltage–current characteristic of a 10-junctions array versus the applied external uniform magnetic field. The parameters chosen are $\alpha = 1$ and $\beta = 2\pi LI_0/\Phi_0 = 2$, where L is the loop inductance, I_0 is the critical current and Φ_0 is the magnetic flux quantum. The external field is varied in a range corresponding to a magnetic flux of 4 flux quanta. The curve for $B = 0$ corresponds to the expected I–V characteristic of an overdamped Josephson junction, implying that all the junctions of the array behave similarly. As the external magnetic field is varied this symmetry is broken and some peculiar features appear: a periodic modulation of the array critical current, and the appearance of a "shoulder" in the I–V curve having maximum amplitude when an odd number of half flux quanta enters the junction. The periodic critical current modulation is the same as a two-junctions interferometer, while the "shoulders" are peculiar features of the array and

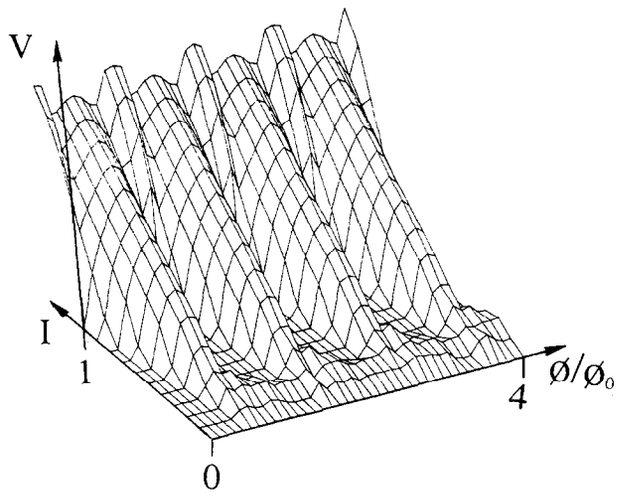

Fig. 5. I–V characteristic of a 10 junctions array vs magnetic field; $\alpha = 1$ and $\beta = 2$.

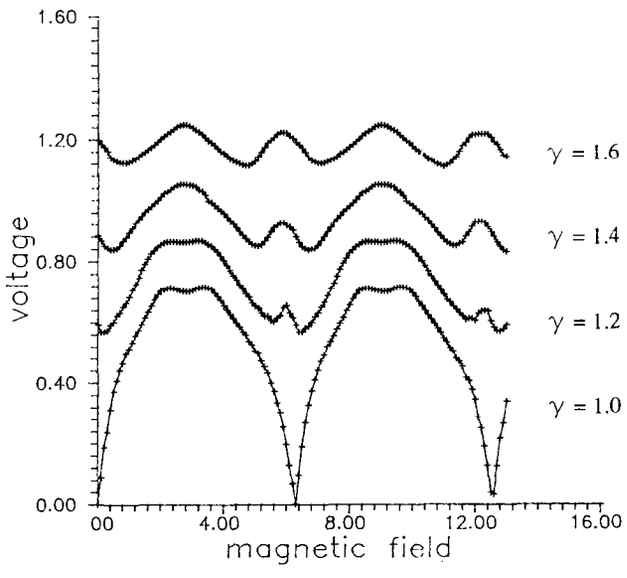

Fig. 6. Array voltage vs magnetic field (in $2\pi\Phi/\Phi_0$ units) at different values of the reduced bias current; $\alpha = 1$ and $\beta = 1$.

correspond to a unidirectional fluxon propagation (flux-flow).

The effect of the flux flow in the array is also shown in Fig. 6, where the dependence of the array voltage on the externally applied magnetic flux is shown for various values of the bias current. The model parameters in this case are $\alpha = 1$ and $\beta = 2$. While, for low bias values, the simple SQUID periodicity of one flux quantum is conserved, when the bias current is increased, the periodicity practically doubles, indicating the occurrence of a more complex dynamic in the array.

What is going on inside the array when the flux-flow state is stimulated can be seen in Fig. 7, where a contour plot of the magnetic field inside the array is shown versus the time and array position. In this case $\alpha = 1, \beta = 5, \gamma = I/I_0 = 0.7$ and $\eta = \Phi/\Phi_0 = 0.5$. In this figure it can be clearly seen how single flux

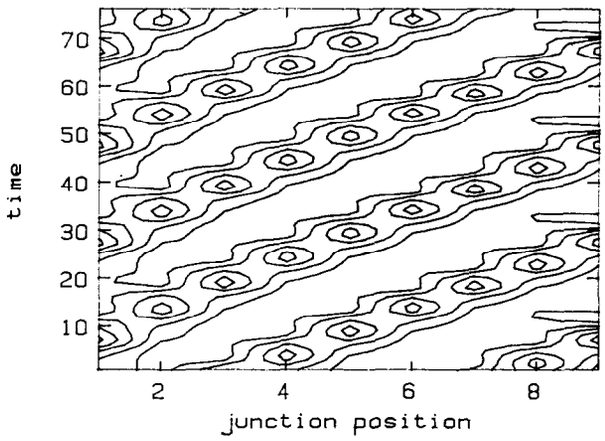

Fig. 7. Contour plot of the magnetic field inside the array when biased in the flux regime; $\alpha = 1$, $\beta = 5$, $\gamma = 0.7$ and $\eta = 0.5$.

quanta are continously injected in the array from the left edge by the external magnetic field, and move from left to right, pushed by the bias current, forming a discontinuous "flux-flow". Indeed the flux motion occurs as a sequence of jumps from one array loop to the next.

The degree of smoothness of this motion is ruled by the value of the parameter β, which is essentially the square of the array loop dimension normalized to the Josephson penetration length λ_j. When $\beta < 1$, a flux quanta, whose size is of the order of λ_j, is spread over more than one loop and consequently its motion is not very sensitive to the discontinuous nature of its propagation medium. When $\beta > 1$, a flux quanta is fully contained in a single array loop, and therefore its motion occurs as a sequence of jumps from one loop to the next.

When a flux quantum reaches the right edge of the array, and a proper load is attached, it is fully absorbed, thus generating a voltage pulse. The sequence of voltage pulses generated by the train of fluxons absorbed represents the signal generated by the oscillator.

As an example of usage of such an oscillator we have simulated the operation of an array, operating in the flux-flow regime, connected by a resistor to a single junction, equal to one of the array junctions, acting as a detector. The resistor models the attenuation of a transmission line that will connect the oscillator to its load in a real device.

In Fig. 8 the I–V curve of the detector junction is shown in two cases: on the left when the array is not biased and no microwave power is generated, and on the right when the array is biased in the flux-flow regime. In the latter case the detector junction shows two clear phase-locked states, at $V = 0.6$ and $V = 1.2$, corresponding to the first sub-harmonic and first Shapiro step.[4] The array

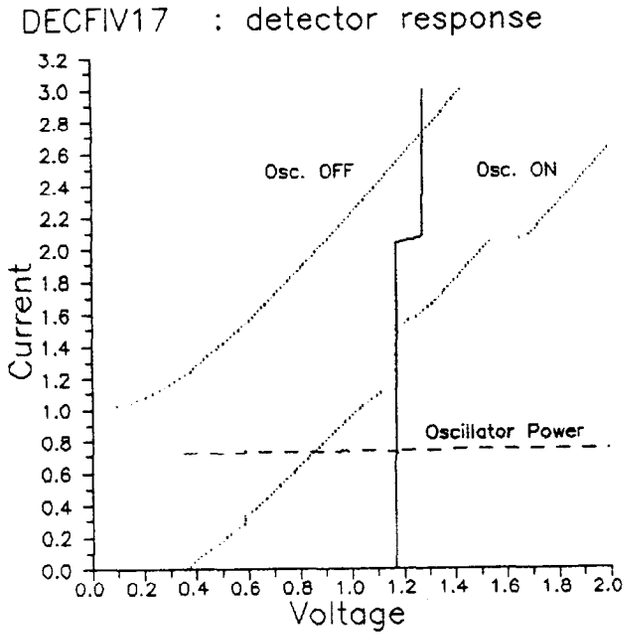

Fig. 8. I–V curve of the detector junction; (left) array is not biased and no microwave power is generated, (right) array is biased in the flux-flow regime.

voltage, which in the flux-flow regime is proportional to the frequency of the generated microwave signal, is shown as a full curve in the figure, and the normalized power emitted is shown as a dashed curve. The shift in the array voltage occurring when the detector bias exceeds 2 is due to the back effect of the detector bias on the array, which is not dc-decoupled.

The results shown in Fig. 8 indicate the possibility of using simple Josephson junction configurations, like the parallel arrays, as useful devices for applications in the microwave field. The device investigated here is essentially a voltage-controlled oscillator operating at a frequency that can be estimated to be up to 100 GHz. The optimization of the emitted power, radiation line-width and frequency is, however, a powerful task that requires a good control of the fabrication technology for the junctions, so as to provide good uniformity of the junction parameters in the array and the possibility of choosing substrates with good microwave properties.

4 CONCLUSIONS

Results concerning high-T_c Josephson devices have been presented. In particular SQUID structures based on a YBCO step-edge junction have been discussed. The results, though far from being conclusive, appear to be quite promising. In addition, the relevant issue of fluxon dynamics in arrays of Josephson junctions has been considered. The dynamics of an array of inductively coupled Josephson junctions have been investigated and its feasibility as a microwave generator when operated in the flux-flow regime is shown. The device can be realized within the present high-T_c junctions technology, and work in this direction is in progress.

ACKNOWLEDGEMENTS

The authors wish to thank G. Costabile, R. Cristiano and R. D. Parmentier for helpful discussions and suggestions and are also indebted to R. Leoni, C. Centioli, U. Baffi and L. Di Virgilio for their contributions. S. P. is grateful to the MIDIT (Denmark) for hospitality during part of this work. The financial supports of the Progetto Finalizzato "Superconducting and Cryogenics Technologies" of the National Research Council (CNR) of Italy and of EEC through Contract No. SC1*-CT91-0760 (TSTS) are acknowledged.

REFERENCES

1. GROSS, R. & CHAUDARI, P., SQUID employing high temperature superconductors. In *Principles and Applications of Superconducting Quantum Interference Devices*, ed. A. Barone. World Scientific, Singapore, 1992.
2. MATARAZZO, S., BARBANERA, S., BOFFA, V., BRUZZESE, R., CICIULLA, F., GAMBARDELLA, U., PENNA, M., MURTAS, F., PAGANO, S. & ROMEO, C., *J. Supercond.*, **6** (1993) 393.
3. ROMEO, C., BOFFA, V., BOLLANTI, S., PATERNÒ, G., ALVANI, C., PENNA, M., BARBANERA, S., CASTRUCCI, P., LEONI, R. & MURTAS, F., *Physica C*, **180** (1991) 77.
4. BARONE, A. & PATERNÒ, G., *Physics and Applications of the Josephson Effect*. John Wiley and Sons Inc., New York, 1982.
5. FULTON, T. A. & DYNES, R. C., *Solid State Commun.*, **12** (1973) 57.
6. McLAUGHLIN, D. W. & SCOTT, A. C., *Phys. Rev.*, **A18** (1978) 1652.
7. PARMENTIER, R. D., Solitons and long Josephson junction. In *The New Superconducting Electronics*, ed. H. Weinstock & Richard W. Ralston. Kluwer Academic Publishers, Dordrecht, The Netherlands, 1993.
8. HONTSU, S., ISHII, J., *J. Appl. Phys.*, **63** (1988) 2021.
9. PAGANO, S., MONACO, R. & COSTABILE, G., *IEEE Trans. Magn*, **MAG-25** (1989) 1080.
10. STERN, J. A., LEDUC, H. G. & ZMUIDZINAS, J., *IEEE Trans. Appl. Supercond.*, **3** (1993) 2485.
11. FILATRELLA, G., MATARAZZO, S. & PAGANO, S., Fluxon dynamics in discrete Sine Gordon system. In *Future Directions of Nonlinear Dynamics in Physical and Biological Systems*, ed. P. L. Christiansen, R. D. Parmentier & C. Eilbeck. Plenum Press, New York, 1993.